Title: Thyroid hormone coordinates developmental trajectories but does not underlie developmental truncation in Danionins

Authors: Yinan Hu, Angela Mauri, Joan Donahue, Rajendra Singh, Benjamin Acosta, Sarah McMenamin

Institutional Affiliation: Boston College Biology Department

Corresponding Contact Information:
Sarah McMenamin
Boston College
Biology Department
140 Commonwealth Ave
Chestnut Hill MA 02467
mcmenams@bc.edu
617-552-3989

Running Title: Thyroid Hormone in Danionins

Key Words: thyroid hormone, zebrafish, Danionella, paedomorphosis, metamorphosis, morphometrics, lateral line, neuromasts

Bullet Points:
• Thyroid hormone regulates shifts in relative growth trajectories in different zebrafish tissues
• Thyroid hormone inhibits head growth in juvenile zebrafish, and regulates juvenile growth patterns
• Thyroid hormone stimulates formation of neuromast canals in the head and 'stitches' on the trunk of zebrafish
• *Danionella*, the miniaturized sister group to *Danio* morphologically resemble larval zebrafish and do not form neuromast canals
• Hypothyroidism is not the cause of paedomorphosis in *Danionella*

Grant Sponsors:
NIH R00GM105874
NIH R03HD091634
Burroughs Wellcome Collaborative Research Travel Grant 1017439

ABSTRACT

Background

Changes in post-embryonic developmental trajectories can profoundly alter adult phenotypes and life history transitions. In vertebrate clades with complex, biphasic life cycles, thyroid hormone (TH) regulates metamorphosis, and alterations to TH metabolism underlie famous cases of paedomorphosis. We tested the requirement for TH in multiple post-embryonic developmental processes in the zebrafish, and asked if TH loss was associated with paedomorphosis in miniaturized *Danionellas*.

Results

We found that TH regulates the relative growth of different body parts in zebrafish, inhibiting head growth at juvenile stages. The lateral line also showed sensitivity to the hormone: head neuromasts were inhibited by TH, while trunk neuromasts required TH for their proliferation. While several aspects of *Danionella* morphology resembled that of larval zebrafish, these species did not resemble hypothyroid zebrafish in their shape or lateral line, and these fish showed functional thyroid follicles.

Conclusions

Although zebrafish do not undergo a discrete ecological transformation, we found that multiple tissues go through a protracted metamorphosis, and that TH ushers in growth patterns and processes typical of juveniles. We found no evidence that compromised TH metabolism is responsible for paedomorphosis in *Danionellas.* Nonetheless, modulations to TH-sensitive pathways affect evolutionarily-relevant traits, and are likely important targets for adaptation.

INTRODUCTION

Shifts in the timing and magnitude of developmental processes during later, post-embryonic stages of development can profoundly alter ultimate phenotypes (Gould 1977, Raff 1996, Smith 2001). Revealing the pathways that regulate trajectories of different developmental processes will be critical in understanding how life histories and phenotypes are formed. Further, discerning how disparate processes may be decoupled will be critical for a complete understanding of the evolution of development.

An extreme way in which post-embryonic development may be changed is through paedomorphosis, wherein an organism does not complete terminal stages of development (Gould 1977, Shaffer and Voss 1996). Organisms on the spectrum of paedomorphosis retain larval characteristics into reproductive maturity (Johnson and Voss 2013). Paedomorphosis is generally most obvious in clades with biphasic (complex) life histories. In these biphasic groups, metamorphosis normally entails a dramatic shift in ecological niche, so paedomorphosis can involve the loss of a markedly divergent life history stage (McMenamin and Hadly 2010, Johnson and Voss 2013). Paedomorphosis in clades with monophasic life cycles may be more ecologically and morphologically subtle, but has nonetheless been posited in many groups, including mammals (e.g. Shea 1983, Goodwin, Bradshaw et al. 1997).

Dramatic, ecological metamorphosis is often initiated by a single molecular signal, so that loss of that pathway could lead to paedomorphosis. Vertebrates with biphasic life cycles, notably anurans and salamanders, experience a metamorphosis stimulated by thyroid hormone (TH; Brown and Cai 2007). Disruptions to TH production or peripheral insensitivity to TH cause developmental arrest, and these changes frequently underlie paedomorphosis, as in the

Mexican axolotl (see Johnson and Voss 2013, De Groef, Grommen et al. 2018). Vertebrates with monophasic life cycles generally have more subtle relationships with the signals that regulate progression through post-embryonic development. Although TH frequently functions as an important regulator of developmental processes in monophasic vertebrates (including zebrafish and mammals), disruptions to the thyroid axis do not result in whole-organism developmental arrest (Brown 1997, Rastogi and LaFranchi 2010, McMenamin, Bain et al. 2014, Buchholz 2015). In these groups, the pathways regulating postembryonic developmental progression are less clear, as are the mechanisms and pathways that may underlie evolutionary paedomorphosis.

Teleosts represent the largest and most speciose group of vertebrates, exhibiting a remarkable range of life history strategies (Finn and Kapoor 2008, McMenamin and Parichy 2013). Numerous teleosts exhibit unequivocally biphasic (or polyphasic) life cycles punctuated by spectacular, ecological metamorphoses. Like in amphibians, metamorphosis in several fishes (notably, flat fish and reef fish) is stimulated by TH. As in other TH-triggered metamorphoses, the hormone stimulates the abrupt transformation of discrete tissues across the body, causing dramatic changes in overall morphology, sensory systems and other organs (Isorna, Obregon et al. 2009, Holzer and Laudet 2015, Holzer, Besson et al. 2017).

Many teleosts, including the zebrafish, do not undergo a discrete ecological transition, and are thus considered to have mono- rather than biphasic life cycles. Nonetheless, the transformations that specific tissues undergo during post-embryonic development—e.g. the pigment pattern (Parichy and Turner 2003, Parichy 2006), and the lateral line (Webb and Shirey 2003)—have been described as metamorphoses. TH has been shown to regulate developmental timing in other monophasic teleosts, particularly their skeletons (Shkil, Borisov et al. 2010, Shkil, Kapitanova et al. 2012). Whether in total these postembryonic transformations constitute a “metamorphosis” essentially depends on how broadly metamorphosis is defined (e.g. see Laudet 2011, McMenamin and Parichy 2013). A clearer picture of the normal developmental trajectories in zebrafish, as well as the relative dependencies on TH, can inform our concept of whether this group exhibits metamorphosis.

Many fish species have been described as paedomorphic, including ice fish (Albertson, Yan et al. 2010), gobies (Johnson and Brothers 1993, Giovannotti, Cerioni et al. 2007) and blennioid fishes (Hastings 2002). *Danionellas* are Danionins relatively closely related to zebrafish (McCluskey and Postlethwait 2014). Members of this miniaturized group are developmentally arrested and resemble larval *Danios* in several ways: adult *Danionellas* lack scales, barbels and many typically late-ossifying bones (Britz, Conway et al. 2009, Britz and Conway 2016), and they retain a larva-like pigment pattern and feeding kinematics (McMenamin, Carter et al. 2017, Galindo, Sweet et al. 2018). *Danionellas* are emerging as a novel model for studying behavior, neurobiology and brain function (Penalva, Bedke et al. 2018, Schulze, Henninger et al. 2018), and a hybrid genome assembly was recently completed (Kadobianskyi, Schulze et al. 2019). A better understanding of the relationships between *Danionellas* and developing zebrafish, along with insights into the pathways that may underlie the group’s remarkable developmental arrest, will inform a better grasp of this emerging model.

In this study we focused on two divergent developmental systems that change over the course of Danionin post-embryonic development. We first focused on shape, which frequently changes dramatically as organisms mature from larva to adult. Organisms with biphasic life

cycles are expected to exhibit considerable shape change (allometric growth) during the metamorphic climax, followed by more proportional (isometric) growth as adults.

We next focused on development of the lateral line. This flow-sensing sensory system consists of individual neuromasts that are broadly distributed across the body (Webb and Shirey 2003, Coombs, Bleckmann et al. 2014, Webb 2014).

Our goals in this study were threefold. First, we aimed to characterize zebrafish shape change and the development of the lateral line during normal zebrafish development, asking whether these developmental trajectories show evidence of a marked metamorphic transformation that corresponds with a period of increased TH production. Second, we tested the requirement for TH in the development of these systems, determining the extent to which TH is required to couple shape change and lateral line development to overall growth. Finally, we tested whether adults of two *Danionella* species recapitulate any stage of normal zebrafish ontogeny, and further tested the possibility that developmental arrest of these species is due to a lack of TH production.

RESULTS AND DISCUSSION

Zebrafish show allometric and proportional shifts during post-embryonic development

In order to determine if zebrafish normally undergo shifts in overall morphology that could be considered a metamorphosis, we first explored the allometric growth trajectories of body shape. Together, the first three principal components capture more than 88% of total shape variation; these were plotted against individuals' SL to visualize how shape changes with growth (Fig 1). PC1 primarily captures body depth (Fig 1D, G). In this axis, EuTH fish allometrically increase body depth until the end of the larval phase (~10mm SL), then maintain a roughly isometric constant body depth (green crosses, Fig 1A). PC2 primarily captures head proportion. This axis peaks at ~9 mm SL, and then decreases gradually during juvenile and adult growth, reflecting (green crosses, Fig 1B). The dorsal profile, captured by PC3, becomes steadily flatter during ontogeny (green crosses, Fig 1C).

To more directly test for changes in head growth during development, we plotted the ratio of head/SL over the course of growth. This ratio showed a similar trend as PC2, with head/SL ratios peaking at ~8 mm SL and then gradually declining (green crosses, Fig 2C). Eyes continued to grow proportionally, peaking at ~10 mm SL (green crosses, Fig 2D). Thus, EuTH zebrafish exhibit shifts in allometric relationships during the transition from larva to juvenile (8-10 mm SL); these shifts are consistent with a systemic metamorphosis. The pattern of positive allometric growth of the head has been documented in a number of fish species (e.g. see Osse, Van den Boogaart et al. 1997, Gisbert 1999, Gisbert and Doroshov 2006), and is generally thought to reflect the strong selection for fish larvae to rapidly develop the craniofacial feeding, respiratory and sensory systems early in their development.

TH inhibits head growth in the juvenile

To determine the extent to which TH was required for these allometric shifts, we measured shape and proportion changes in a TH- background. Changes in body depth were insensitive to TH, and shape changes in the PC1 axis were indistinguishable between the two treatments (Fig 1A). However, we found that TH influences the relative growth of the head: when TH is absent, PC2 continues to increase along a larva-like trajectory until ~10 mm SL (purple circles, Fig 1B).

The third PC axis reveals that TH- fish acquire a flatter dorsal profile, unlike that of any stage of EuTH development (Fig 1C).

In the absence of TH, heads and eyes continue to grow along a relatively steeper (larva-like) trajectories (Fig 2A, B). After the rapid relative growth during larval development, the relative size of the head and eye does not decline appropriately in TH- backgrounds (Fig 2C-D). Thus, TH is required for the coordinated transition from a larval trajectory to the juvenile trajectory, and is in particular required to limit the relative growth of the head in juveniles.

TH inhibits proliferation of head neuromasts, but promotes formation of neuromast 'stitches' on the body

We next examined the development of a trait that emerges by very different mechanisms than body morphology. We tracked numbers of neuromasts of the lateral line across a range of body sizes. In EuTH fish, the number of trunk neuromasts increases roughly in proportion to growth, whereas head neuromasts show a negative allometric relationship to body size (green crosses, Fig 3A, J; Supplementary Fig 1). We found that TH- adults showed ~25% more total neuromasts than EuTH adults (Supplementary Fig 1A), and that this difference was driven primarily by the increasing population of head neuromasts (Fig 3A). This increase in head neuromast number is not simply due to the larger heads of TH- fish, as the differences remain even when standardized to head length (Supplementary Fig 1B). A subset of head neuromasts in EuTH eventually sink into bony canals and acquire an elongated, rod-like shape (Webb and Shirey 2003). We found that although neuromasts do become enclosed in canals in TH- adults, these canal-neuromasts fail to acquire the mature morphology as seen in EuTH adults (Fig 3, Supplementary Fig 2). It is possible that transition into mature canal neuromasts serves as the cue to inhibit proliferation among the superficial neuromasts, and therefore TH- head neuromasts remain highly proliferative through adulthood.

In EuTH fish, vertical series of neuromasts on the trunk, referred to as 'stitches' (Ledent 2002), begin to form when fish are ~10 mm SL. In the TH- trunk, the neuromast population grows at a retarded rate until stitches start forming at ~13 mm SL (Fig 3J), suggesting TH regulates the relative timing of stitch formation.

Bioavailability of TH shifts during mid-larval development

TH production peaks during metamorphic climax in amphibians, measured as both the prohormone T4 (the form of TH primarily produced by the thyroid gland) and the more biologically active T3, converted by peripheral deiodinases 1 and 2 (Regards, Taurog et al. 1978, Kikuyama, Kawamura et al. 1993, Shi 2000, Brown and Cai 2007). We wanted to test whether the TH-stimulated physiological changes in zebrafish corresponded with elevated TH production or changes in the ratio of T3/T4. We measured T4 and T3 levels at seven stages from larval through juvenile development, staging groups of fish according to the Standardized Standard Length staging criteria (SSL; Parichy, Elizondo et al. 2009). The relative levels of T3 and T4 remained relatively consistent from one stage to another, except as fish transitioned from 6 to 6.4 SSL. During this period, when anal and dorsal rays first appear (Parichy, Elizondo et al. 2009), we detected a drop in T4 corresponding with an increase in T3 titer (Fig 4A-C). We conclude that there is a shift in TH bioavailability during this mid-larval period, which we have

highlighted with grey bars in all of our graphs (Figs 1-4). Following this shift, T3 availability remained elevated through juvenile development (Fig 4B).

A previous analysis identified a similar shift in T3/T4 ratio at 10-14 dpf, attributed to higher deiodinase activity (Chang, Wang et al. 2012). Indeed, while expression of *thyroglobulin* remains relatively stable from 10-20 dpf, *deiodinase 2* expression increases twofold (Vergauwen, Cavallin et al. 2018). However, these patterns are difficult to perfectly correlate with our measurements, as dpf (used in these previous analyses) is a poor proxy for size and developmental stage (Parichy, Elizondo et al. 2009, McMenamin, Chandless et al. 2016).

The mid-larval shift in the T3/T4 ratio occurs at a smaller size (6.4 mm SL) than when shifts occur in developmental trajectories in EuTH fish (8-10 mm SL; Figs 1-2), and TH- fish do not begin to diverge from EuTH fish until ~8mm SL (Fig 2B, Fig 3). Therefore, a direct link between these shifts and the change in T3/T4 ratio seems unlikely. T3 may effect changes in progenitor cell fates during the mid-larval period; these changes may influence long-term growth of different tissues such that the morphological effects are not apparent in the proportions of the fish after several more mm of growth. Alternatively, prolonged exposure to the hormone may be required to effect morphological changes. Regardless, TH- zebrafish maintain inappropriately longer periods of larval growth patterns, resulting in fish that do not maintain larval shapes, but achieve novel adult phenotypes.

Adult *Danionellas* resemble larval zebrafish morphology

Danionellas maintain numerous characteristics of larval *Danios*, and are described as paedomorphic (Britz, Conway et al. 2009, Britz and Conway 2016). We thus tested the prediction that *Danionella* body shape would more closely resemble larval than adult zebrafish, reanalyzing morphometric datasets to include two species of *Danionella*. *Danionella* adults of both species showed lower PC1 scores than similarly-sized zebrafish (blue triangles and orange squares, Supplementary Fig S3), reflecting immature (i.e. paedomorphic) shapes relative to similarly-sized zebrafish. *Danionella*s also showed proportionally smaller heads and eyes for their body length (blue triangles and orange squares, Fig 2). Thus, *Danionellas* indeed maintain certain morphologies similar to those of larval *Danios*, and likely show much more isometric patterns of growth during development.

Although *D. translucida* were smaller than *D. priapus*, the two species showed similar absolute numbers of neuromasts (Supplementary Fig S1A). *D. priapus* showed neuromast numbers comparable to those of similarly-sized EuTH zebrafish, while *D. translucida* showed more neuromasts, with a greater density in the trunk (Fig 3, Supplementary Fig S1A; Supplementary Fig S4).

***Danionellas* do not show a morphological signature of hypothyroidism and have functioning thyroid follicles**

Since TH is involved in the most famous examples of paedomorphosis (Gould 1977, Johnson and Voss 2013, De Groef, Grommen et al. 2018) , we wanted to test the possibility that TH metabolism was disrupted in *Danionellas*. First, we asked if *Danionellas* appeared more similar to TH- than to EuTH zebrafish. In terms of morphometrics (Supplementary Fig 3) and ratios of head and eye to SL (Fig 2), both *Danionella* species actually more closely resembled similarly-sized EuTH than TH- zebrafish. Contrary to the pattern observed in TH- zebrafish, *Danionellas*

show fewer head neuromasts and more trunk neuromasts than similarly-sized EuTH zebrafish. However, like TH- zebrafish, *Danionellas* were not found to possess any elongated canal neuromasts (Fig 3 E, I). Overall, in terms of body shape and lateral line distribution, *Danionellas* did not resemble TH- zebrafish. To further confirm that hypothyroidism did not underlie developmental truncation in these species, we examined the thyroid follicles, which we found to be intact and expressing T4 (Fig 4E-F).

Conclusions

We identified shifts in allometric trajectories as EuTH zebrafish transition from larvae to juveniles; these shifts are fundamentally different from typical metamorphosis seen in biphasic species, but we interpret this as a protracted and 'cryptic' metamorphosis. We found that some aspects of these shifts are TH-dependent, and that in the absence of the hormone, fish continue along larval allometric trajectories to inappropriate sizes. Further, TH stimulates the formation of canal neuromasts and lateral line stitches, processes that normally occur during the larva-to-juvenile transition. However, unlike hypothyroid amphibians, which maintain larval morphology through adulthood, TH- zebrafish inappropriately maintain larval growth trajectories to achieve novel adult phenotypes. We conclude that TH normally coordinates the transition from larval to juvenile developmental programs in zebrafish.

Consistent with the idea that *Danionellas* are paedomorphic, two *Danionella* species showed proportional similarities to larval zebrafish, and also failed to develop facial canal neuromasts typical of adult zebrafish. These paedomorphs bore little resemblance to TH-zebrafish, and we found that they produced T4. We conclude that, unlike in paedomorphic amphibians, disruptions to the thyroid axis do not cause paedomorphosis in these species.

EXPERIMENTAL PROCEDURES

Fish rearing

All zebrafish are from the transgenic zebrafish line *tg:nVenus-v2a-nfnB* (McMenamin et al. 2014). Transgenic fish were treated 4-5 days post fertilization (dpf) with DMSO (for control EuTH) or DMSO + metronidazole (for thyroid ablation, TH-), following McMenamin et al (2014). Fish were reared under TH-free conditions with a diet of rotifers, *Artemia* and pure spirulina flakes (Pentair) at 28°C with 12:12 light:dark cycles, and fed three times per day. *Danionella translucida* were a gift from Adam Douglass, University of Utah; *D. priapus* were purchased through The Wet Spot (Portland OR). *Danionellas* were fed rotifers, *Artemia* and Gemma micro (Skretting).

Quantification of thyroxine (T4) and triiodothyronine (T3)

Live wild-type zebrafish were anesthetized and staged following the adult normal table (Parichy et al. 2009). Seven stages were chosen to capture major processes during the entire larva-to-juvenile transition (see Supplemental Table 1), and fish were staged by the SSL convention (Parichy, Elizondo et al. 2009). Samples were prepared following McMenamin et al. (2014). Staged fish were pooled, euthanized by tricaine overdose, blotted dry, and weighed in microcentrifuge tubes. Tissue was suspended in cold methanol with 1 mM 6-propyl-2- thiouracil (PTU; Sigma) and homogenized by sonication; homogenized samples were stored at -80°C until analysis. Samples were centrifuged, re-extracted with additional PTU-containing methanol.

Supernatants were pooled and dried with a CentriVap Concentrator (Labconco) for ~5 hours, then resuspended in PBS. Samples were run on T4 and T3 ELISA kits (Diagnostic Automation Inc.) with two technical replicates and with three biological replicates for each stage. Plates were analyzed on a PerkinElmer Victor X5; mean absorbance value from three readings was used for subsequent analysis. Standard curves were generated with 4-parameter logistic regression via online analysis software (www.elisaanalysis.com).

Live staining of neuromasts

4-(4-Diethylaminostyryl)-1-methylpyridinium iodide (DiASP, AdipoGen) was used to visualize neuromasts (Collazo, Fraser et al. 1994). Individual fish were incubated in 0.0024% DiASP in fish system water with 0.02% tricane for 5 minutes, then transferred to 2% methylcellulose and imaged with an Olympus DP74 camera mounted on an Olympus SZX16 stereoscope. Standard length (SL) was measured using ImageJ (Schneider, Rasband et al. 2012). Neuromasts were counted manually from digital images; all counts were all performed by the same individual to reduce variability.

Scanning Electron Microscopy

TH- and EuTH adults were fixed in 4% paraformaldehyde (Sigma) overnight at 4°C, rinsed several times with PBS, and dehydrated in an ascending series of ethanol. Samples were critical point dried in 100% ethanol, coated with Au-Pd and imaged with a JEOL JCM-6000PLUS NeoScope Benchtop SEM.

Fixation and skeletal staining

Specimens were euthanized by overdose of Tricane (Western Chemical), then fixed in 4% paraformaldehyde (Sigma) overnight at 4°C. Specimens were rinsed several times with PBS and dehydrated in 70% ethanol. Following (Walker and Kimmel 2007), skeletons were stained overnight in 0.5% Alizarin red (Sigma) and 0.02% Alcian Blue (Sigma) with 60 mM $MgCl_2$ in 70%. Stained specimens were bleached with 3% hydrogen peroxide in 1% potassium hydroxide (KOH) until melanocytes turned brown, then were cleared by gradually transitioning through an ascending glycerol series from 25% to 80%. Prior to imaging, cleared specimens were incubated in PBS overnight, and then transferred into 2% methylcellulose for positioning and imaged as above for morphometric analysis.

Morphometrics

Homologous anatomical landmarks and curves that outline the body were placed manually (by a single individual) on lateral images of fish using the R package Stereomorph (Olsen and Westneat 2015). A list of the specific landmarks can be found in the supplementary materials (supplementary Table S1). Landmark data was then analyzed with standard geometric morphometrics methods using the R package Geomorph (Adams and Otárola-Castillo 2013).

Head size and eye size.

Size was measured on lateral images of cleared and stained specimens. Head size was measured as the distance from the tip of the snout/rostral edge of premaxilla to the posterior tip of the occipital. For the eye, two measurements, the dorsal-ventral height, and the anterior-

posterior length were obtained, and then averaged as the eye-size measure. Measurements were performed by a single individual to reduce variability.

Thyroid staining

To image thyroid follicles, adult *D. rerio*, *D. priapus* and *D. translucida* were fixed in 4% paraformaldehyde (Sigma), embedded in O.C.T. Compound (Fisher Scientific), and sectioned by cryostat to 12 µm. Sections were washed with 0.1% tween in PBS (PBSt), blocked with 10% heat-inactivated goat serum in PBSt, then incubated at 4°C overnight with a rabbit T4 antibody (1:1000, Fitzgerald). Slides were then washed, incubated with a secondary antibody (goat anti-rabbit FITC diluted 1:1000, Fitzgerald), stained with DAPI (1ug/ml) for 20 minutes, washed and imaged on an Olympus IX83 microscope equipped with a Hamamatsu ORCA Flash 4.0LT camera.

Statistics

All statistical analyses were performed in in R (version 3.4.1). Differences in thyroid hormone levels along ontogeny were first examined using ANOVA, followed by Tukey's honest significant distance test. Developmental trajectory was estimated with the spm function under package SemiPar using default settings (Carroll, Ruppert et al. 2003).

ACKNOWEDGEMENTS

Thank you for technical support and comments from Catherine May, Stacy Nguyen, Pranav Parikh, Mary Xu and all the members of the McMenamin Lab. Thanks to the Boston College Animal Care Facility staff for support with fish rearing. Thanks to Adam Douglass for *Danionella* samples. We gratefully acknowledge support from NIH R00GM105874, R03HD091634 and Burroughs Wellcome Grant 1017439.

REFERENCES

Adams, D. C. and E. Otárola-Castillo (2013). "geomorph: an R package for the collection and analysis of geometric morphometric shape data." Methods in Ecology and Evolution **4**(4): 393-399.

Albertson, R. C., Y.-L. Yan, T. A. Titus, E. Pisano, M. Vacchi, P. C. Yelick, H. W. Detrich and J. H. Postlethwait (2010). "Molecular pedomorphism underlies craniofacial skeletal evolution in Antarctic notothenioid fishes." BMC evolutionary biology **10**(1): 4.

Britz, R. and K. W. Conway (2016). "Danionella dracula, an escape from the cypriniform Bauplan via developmental truncation?" Journal of morphology **277**(2): 147-166.

Britz, R., K. W. Conway and L. Rüber (2009). "Spectacular morphological novelty in a miniature cyprinid fish, Danionella dracula n. sp." Proceedings of the Royal Society of London B: Biological Sciences **276**(1665): 2179-2186.

Brown, D. D. (1997). "The role of thyroid hormone in zebrafish and axolotl development." Proceedings of the National Academy of Sciences **94**(24): 13011-13016.

Brown, D. D. and L. Cai (2007). "Amphibian metamorphosis." Developmental biology **306**(1): 20.

Buchholz, D. R. (2015). "More similar than you think: Frog metamorphosis as a model of human perinatal endocrinology." Developmental biology **408**(2): 188-195.

Carroll, R., D. Ruppert and M. Wand (2003). Semiparametric regression, Cambridge: Cambridge University Press.

Chang, J., M. Wang, W. Gui, Y. Zhao, L. Yu and G. Zhu (2012). "Changes in thyroid hormone levels during zebrafish development." Zoological science **29**(3): 181-184.

Collazo, A., S. E. Fraser and P. M. Mabee (1994). "A dual embryonic origin for vertebrate mechanoreceptors." Science **264**(5157): 426-430.

Coombs, S., H. Bleckmann, R. R. Fay and A. N. Popper (2014). The lateral line system, Springer.

De Groef, B., S. V. Grommen and V. M. Darras (2018). "Forever young: endocrinology of paedomorphosis in the Mexican axolotl (Ambystoma mexicanum)." General and comparative endocrinology.

Finn, R. N. and B. Kapoor (2008). Fish larval physiology, Science Publishers, Inc.

Galindo, D., E. Sweet, Z. DeLeon, M. Wagner, A. DeLeon, C. Carter, S. McMenamin and W. J. Cooper (2018). "Thyroid hormone modulation during zebrafish development recapitulates evolved diversity in danionin jaw protrusion mechanics." bioRxiv (Preprint) **418483**.

Giovannotti, M., P. N. Cerioni, M. La Mesa and V. Caputo (2007). "Molecular phylogeny of the three paedomorphic Mediterranean gobies (Perciformes: Gobiidae)." Journal of Experimental Zoology Part B: Molecular and Developmental Evolution **308**(6): 722-729.

Gisbert, E. (1999). "Early development and allometric growth patterns in Siberian sturgeon and their ecological significance." Journal of Fish Biology **54**(4): 852-862.

Gisbert, E. and S. I. Doroshov (2006). "Allometric growth in green sturgeon larvae." Journal of Applied Ichthyology **22**: 202-207.

Goodwin, D., J. W. Bradshaw and S. M. Wickens (1997). "Paedomorphosis affects agonistic visual signals of domestic dogs." Animal Behaviour **53**(2): 297-304.

Gould, S. J. (1977). Ontogeny and phylogeny, Harvard University Press.

Hastings, P. A. (2002). "Evolution of morphological and behavioral ontogenies in females of a highly dimorphic clade of blennioid fishes." Evolution **56**(8): 1644-1654.

Holzer, G., M. Besson, A. Lambert, L. François, P. Barth, B. Gillet, S. Hughes, G. Piganeau, F. Leulier and L. Viriot (2017). "Fish larval recruitment to reefs is a thyroid hormone-mediated metamorphosis sensitive to the pesticide chlorpyrifos." Elife **6**: e27595.

Holzer, G. and V. Laudet (2015). "Thyroid hormones: a triple-edged sword for life history transitions." Current Biology **25**(8): R344-R347.

Isorna, E., M. J. Obregon, R. M. Calvo, R. Vázquez, C. Pendón, J. Falcón and J. A. Muñoz-Cueto (2009). "Iodothyronine deiodinases and thyroid hormone receptors regulation during flatfish (Solea senegalensis) metamorphosis." Journal of Experimental Zoology Part B: Molecular and Developmental Evolution **312**(3): 231-246.

Johnson, C. K. and S. R. Voss (2013). Salamander paedomorphosis: linking thyroid hormone to life history and life cycle evolution. Current topics in developmental biology, Elsevier. **103:** 229-258.

Johnson, D. G. and E. B. Brothers (1993). "Schindleria: A Paedomorphic Goby (Teleostei: Aobioidei)." Bulletin of Marine Science **52**(1): 441-471.

Kadobianskyi, M., L. Schulze, M. Schuelke and B. Judkewitz (2019). "Hybrid genome assembly and annotation of Danionella translucida, a transparent fish with the smallest known vertebrate brain." bioRxiv: 539692.

Kikuyama, S., K. Kawamura, S. Tanaka and K. Yamamoto (1993). Aspects of amphibian metamorphosis: hormonal control. International review of cytology, Elsevier. **145:** 105-148.
Laudet, V. (2011). "The origins and evolution of vertebrate metamorphosis." Current Biology **21**(18): R726-R737.
Ledent, V. (2002). "Postembryonic development of the posterior lateral line in zebrafish." Development **129**(3): 597-604.
McCluskey, B. M. and J. H. Postlethwait (2014). "Phylogeny of zebrafish, a “model species,” within Danio, a “model genus”." Molecular Biology and Evolution **32**(3): 635-652.
McMenamin, S., C. Carter and W. J. Cooper (2017). "Thyroid Hormone Stimulates the Onset of Adult Feeding Kinematics in Zebrafish." Zebrafish **14**(6): 517-525.
McMenamin, S., M. Chandless and D. Parichy (2016). Working with zebrafish at postembryonic stages. Methods in cell biology, Elsevier. **134:** 587-607.
McMenamin, S. K., E. J. Bain, A. E. McCann, L. B. Patterson, D. S. Eom, Z. P. Waller, J. C. Hamill, J. A. Kuhlman, J. S. Eisen and D. M. Parichy (2014). "Thyroid hormone–dependent adult pigment cell lineage and pattern in zebrafish." Science: 1256251.
McMenamin, S. K. and E. A. Hadly (2010). "Developmental dynamics of Ambystoma tigrinum in a changing landscape." BMC ecology **10**(1): 10.
McMenamin, S. K. and D. M. Parichy (2013). Metamorphosis in teleosts. Current topics in developmental biology, Elsevier. **103:** 127-165.
Olsen, A. M. and M. W. Westneat (2015). "StereoMorph: an R package for the collection of 3D landmarks and curves using a stereo camera set-up." Methods in Ecology and Evolution **6**(3): 351-356.
Osse, J., J. Van den Boogaart, G. Van Snik and L. Van der Sluys (1997). "Priorities during early growth of fish larvae." Aquaculture **155**(1-4): 249-258.
Parichy, D. M. (2006). "Evolution of danio pigment pattern development." Heredity **97**(3): 200.
Parichy, D. M., M. R. Elizondo, M. G. Mills, T. N. Gordon and R. E. Engeszer (2009). "Normal table of postembryonic zebrafish development: staging by externally visible anatomy of the living fish." Developmental dynamics **238**(12): 2975-3015.
Parichy, D. M. and J. M. Turner (2003). "Zebrafish puma mutant decouples pigment pattern and somatic metamorphosis." Developmental biology **256**(2): 242-257.
Penalva, A., J. Bedke, E. S. B. Cook, J. P. Barrios, E. P. L. Bertram and A. D. Douglass (2018). "Establishment of the miniature fish species *Danionella translucida* as a genetically and optically tractable neuroscience model." bioRxiv: 444026.
Raff, R. (1996). The Shape of Life: Genes, Development and the Evolution of Animal Form, University of Chicago Press.
Rastogi, M. V. and S. H. LaFranchi (2010). "Congenital hypothyroidism." Orphanet journal of rare diseases **5**(1): 17.
Regards, E., A. Taurog and T. Nakashima (1978). "Plasma thyroxine and triiodothyronine levels in spontaneously metamorphosing *Rana catesbeiana* tadpoles and in adult anuran amphibia." Endocrinology **102**(3): 674-684.
Schneider, C. A., W. S. Rasband and K. W. Eliceiri (2012). "NIH Image to ImageJ: 25 years of image analysis." Nature methods **9**(7): 671.

Schulze, L., J. Henninger, M. Kadobianskyi, T. Chaigne, A. I. Faustino, N. Hakiy, S. Albadri, M. Schuelke, L. Maler and F. Del Bene (2018). "Transparent Danionella translucida as a genetically tractable vertebrate brain model." Nature methods **15**(11): 977.

Shaffer, H. B. and S. R. Voss (1996). "Phylogenetic and Mechanistic Analysis of A Developmentally Integrated Character Complex: Alternate Life History Modes in Ambystomatid Salamanders." American Zoologist **36**(1): 24-35.

Shea, B. T. (1983). "Paedomorphosis and neoteny in the pygmy chimpanzee." Science **222**(4623): 521-522.

Shi, Y.-B. (2000). Amphibian metamorphosis, Wiley-Liss.

Shkil, F., V. Borisov, B. Abdissa and S. Smirnov (2010). "Role of thyroid hormone in the ontogeny and morphological diversification of Barbus intermedius sensu Banister, 1973 of Lake Tana in Ethiopia." Russian journal of developmental biology **41**(6): 369-380.

Shkil, F., D. Kapitanova, V. Borisov, B. Abdissa and S. Smirnov (2012). "Thyroid hormone in skeletal development of cyprinids: effects and morphological consequences." Journal of Applied Ichthyology **28**(3): 398-405.

Smith, K. K. (2001). "Heterochrony revisited: the evolution of developmental sequences." Biological Journal of the Linnean Society **73**(2): 169-186.

Vergauwen, L., J. E. Cavallin, G. T. Ankley, C. Bars, I. J. Gabriëls, E. D. Michiels, K. R. Fitzpatrick, J. Periz-Stanacev, E. C. Randolph and S. L. Robinson (2018). "Gene transcription ontogeny of hypothalamic-pituitary-thyroid axis development in early-life stage fathead minnow and zebrafish." General and comparative endocrinology.

Walker, M. and C. Kimmel (2007). "A two-color acid-free cartilage and bone stain for zebrafish larvae." Biotechnic & Histochemistry **82**(1): 23-28.

Webb, J. F. (2014). Lateral line morphology and development and implications for the ontogeny of flow sensing in fishes. Flow Sensing in Air and Water, Springer.

Webb, J. F. and J. E. Shirey (2003). "Postembryonic development of the cranial lateral line canals and neuromasts in zebrafish." Developmental Dynamics **228**(3): 370-385.

FIGURE LEGENDS

Figure 1. Thyroid hormone regulates allometric trajectories in zebrafish. A-C, Principle component (PC) scores of body shape plotted against standard length for both EuTH (green cross) and TH- (purple open circle) individuals. Percent variation explained by each PC axis is shown in upper left. Developmental trajectory is shown in solid line for EuTH and dashed line for TH-. Colored shading shows standard error in the model of developmental trajectory. Grey stripe shows period from 6-6.4 SL, for comparison with other figures. D-F, deformation grids showing extreme shapes along each PC. G-I, vector plots showing shape change along each PC axis, with arrows pointing from negative to positive PC values.

Figure 2. Thyroid hormone regulates body proportions in zebrafish. **A**, head length as a function of SL; **B**, eye diameter as a function of SL. **C**, Head length/SL and **D**, eye diameter/SL as functions of SL. Showing both EuTH (green cross) and TH- (purple open circle) zebrafish, with comparison to *D. priapus* (orangesquare) and *D. translucida* (blue triangle) adults. For zebrafish, developmental trajectory is shown in solid line for EuTH and dashed line for TH-. Colored

shading shows standard error in the model of developmental trajectory. Grey stripe shows period from 6-6.4 mm SL, for comparison with other figures.

Figure 3. Thyroid hormone regulates lateral line development in zebrafish. **A**, Total number of head neuromasts, as a function of SL, with comparison to *D. priapus* (orange square) and *D. translucida* (blue triangle) adults. For zebrafish, developmental trajectory is shown in solid line for EuTH and dashed line for TH-. Colored shading shows standard error in the model of developmental trajectory. Grey stripe shows period from 6-6.4 mm SL, for comparison with other figures. **B-C**, DiASP live staining of facial neuromasts in EuTH juvenile (13 mm SL) and adult (18+ mm SL). Arrowhead indicates rod-shaped canal neuromasts at adult stage. **D**, Scanning electron micrographs of a supraorbital canal neuromast in EuTH adult. Dotted line outlines the neuromast. Solid line outlines the bony edge of the canal. **E**, facial neuromasts in *D. priapus* adult. **F-H**, same as B-D in TH- fish. **I**, facial neuromasts in *D. translucida* adult. **J**, same as A for trunk neuromasts. **K-P**, DiASP live staining of trunk neuromasts in EuTH juvenile (13 mm SL, **K**), EuTH adult (18+mm SL, **L**), *D. priapus* adult (**M**), TH- juvenile (13 mm SL, **N**) TH- adult (18+mm SL, **O**), and *D. translucida* adult (**P**).

Figure 4. Relative thyroid hormone content during larval development in zebrafish. **A**, T4, thyroxine; **B**, T3, triiodothyronine; **C**, ratio of T3 to T4. All concentrations standardized to body weight. Whiskers represents standard error at each stage. Stages that are not statistically different (as determined by Tukey's Honest Significant Differences Test) are represented with the same letter. Grey stripe shows period from 6-6.4 SSL, for comparison with other figures. **D-F**: Antibody staining of T4 in *D. rerio, D. priapus* and *D. translucida* adults showing functional thyroid follicles. Images show 12 uM transverse sections of the thyroid region.

Supplementary Figure S1. Thyroid hormone regulates lateral line development in zebrafish. **A**, Total number of
neuromasts as a function of SL, with comparison to *D. priapus* (orange square) and *D. translucida* (blue triangle) adults. For Danio, developmental trajectory is shown in solid line for EuTH and dashed line for TH-. Colored shading shows standard error in the model of developmental trajectory. Grey stripe shows period from 6-6.4 mm SL, for comparison with other figures. **B**, same as A for head neuromasts divided by head length. **C**, same as B for trunk neuromasts divided by trunk length.

Supplementary Figure S2. Thyroid hormone is required for canal neuromast development. **A-B**, DiASP live staining of facial neuromasts, dorsal view. **A**, EuTH juvenile (11 mm SL); **B**, TH- juvenile (11 mm SL). White arrowheads show supraorbital canal neuromast that has started to elongate. **C-J**, Scanning electron micrographs of supraorbital canal neuromast, each row shown in increasing magnification. White rectangle outlines region shown in the next picture. **C-F**, EuTH adult (18mm+ SL); **G-J**, TH- adult (18mm+ SL).

Supplementary Figure S3. Developmental trajectory of body shape in EuTH and TH- zebrafish, with comparison to *D. priapus* and *D. translucida*. **A-C**, Principle component (PC) scores of body shape plotted against standard length for both EuTH (cross) and TH- (open circle) individuals,

with comparison to *D. priapus* (orange square) and *D. translucida* (blue triangle) adults. Percent variation explained by each PC axis is shown on the upper left corner. Developmental trajectory is shown in solid line for EuTH and dashed line for TH-. Colored shading shows standard error in the model of developmental trajectory. Grey stripe shows period from 6-6.4 mm SL, for comparison with other figures. **D-F**, deformation grids showing extreme shapes along each PC. **G-I**, vector plots showing shape change along each PC axis, with arrows pointing from negative to positive PC values.

Supplementary Figure S4. Neuromast distribution in *Danionella* adults. DiASP live staining of facial neuromasts in **A**, *D. priapus* dorsal view. **B**, *D. priapus* lateral view. **C**, *D. translucida* dorsal view. **D**, *D. translucida* lateral view. Each panel is composed of multiple images digitally combined.

Supplementary Table S1. Landmarks used in morphometric body shape analysis.

	Landmarks
1	Tip of snout/rostral edge of premaxilla
2	Posterior tip of supraoccipital crest
3	Dorsal insertion of the caudal fin
4	Ventral insertion of the caudal fin
5	Point of maximum curvature on the most ventral branchiolstegal ray
	Semi-landmarks
	ventral outline of the head connecting Landmark #1 and #5, n=8
	dorsal outline of the head connecting Landmark #1 and #2, n=8
	dorsal edge of the body connecting Landmark #2 and #3, n=18

Supplementary Table S2. Summary of fish samples used for ELISA.

SSL	Stage	SL (mm)	Age (± SD)	n	average weight (g) per fish
4.9	CR	4.9-5.1	12 ± 2.9	1318	0.000893649
6	aSB	5.9-6.2	13.5 ± 2.5	654	0.001709021
6.4	DR	6.4-6.6	15 ± 2.5	403	0.003138213
7.2	PB	7.2-7.5	16 ± 2.7	294	0.004842177
8.6	PR	8.5-8.7	20 ± 1.3	149	0.008157047
9.8	SP	9.5-9.6	26.5 ± 2.1	98	0.013067347
11	J	10.9-11.7	32 ± 0.5	58	0.022691379

Fig 1

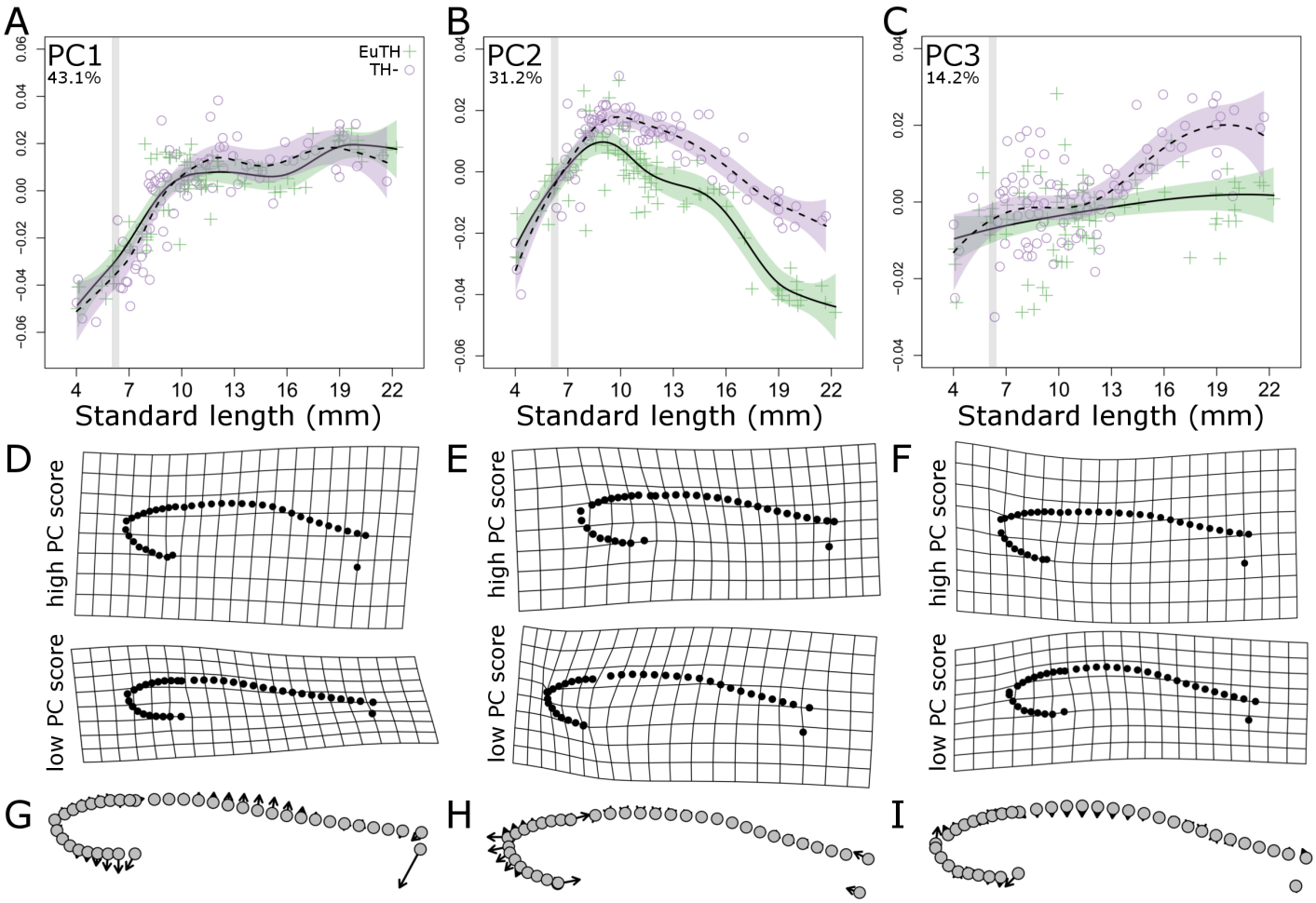
A
PC1
43.1%
EuTH
TH-
Standard length (mm)
B
PC2
31.2%
Standard length (mm)
C
PC3
14.2%
Standard length (mm)
D
high PC score
low PC score
E
high PC score
low PC score
F
high PC score
low PC score
G
H
I

Fig 2

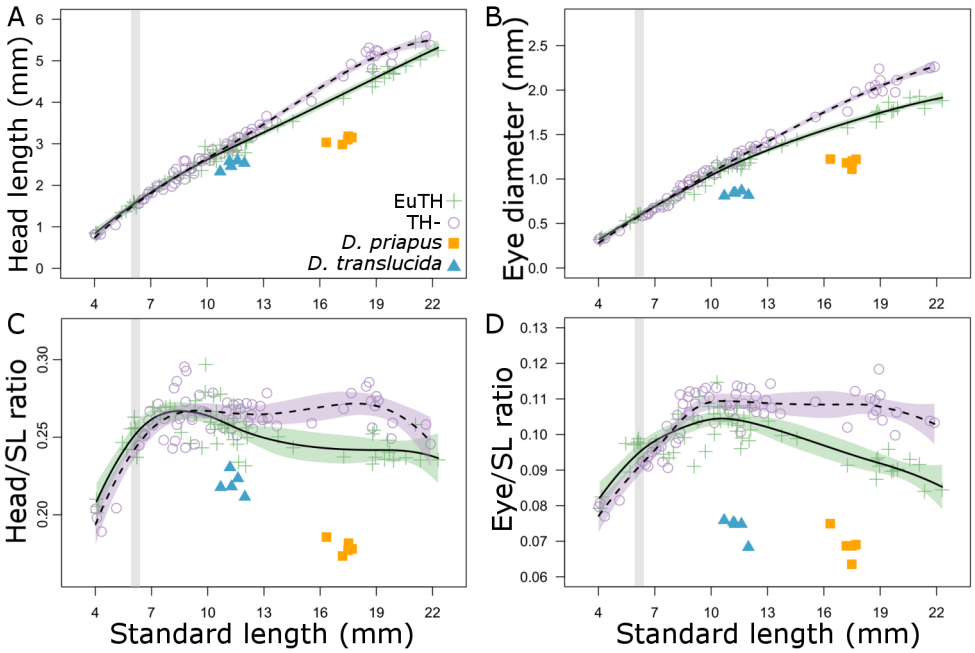
A
Head length (mm)
EuTH
TH-
D. priapus
D. translucida
B
Eye diameter (mm)
C
Head/SL ratio
D
Eye/SL ratio
Standard length (mm)
Standard length (mm)

Fig 3

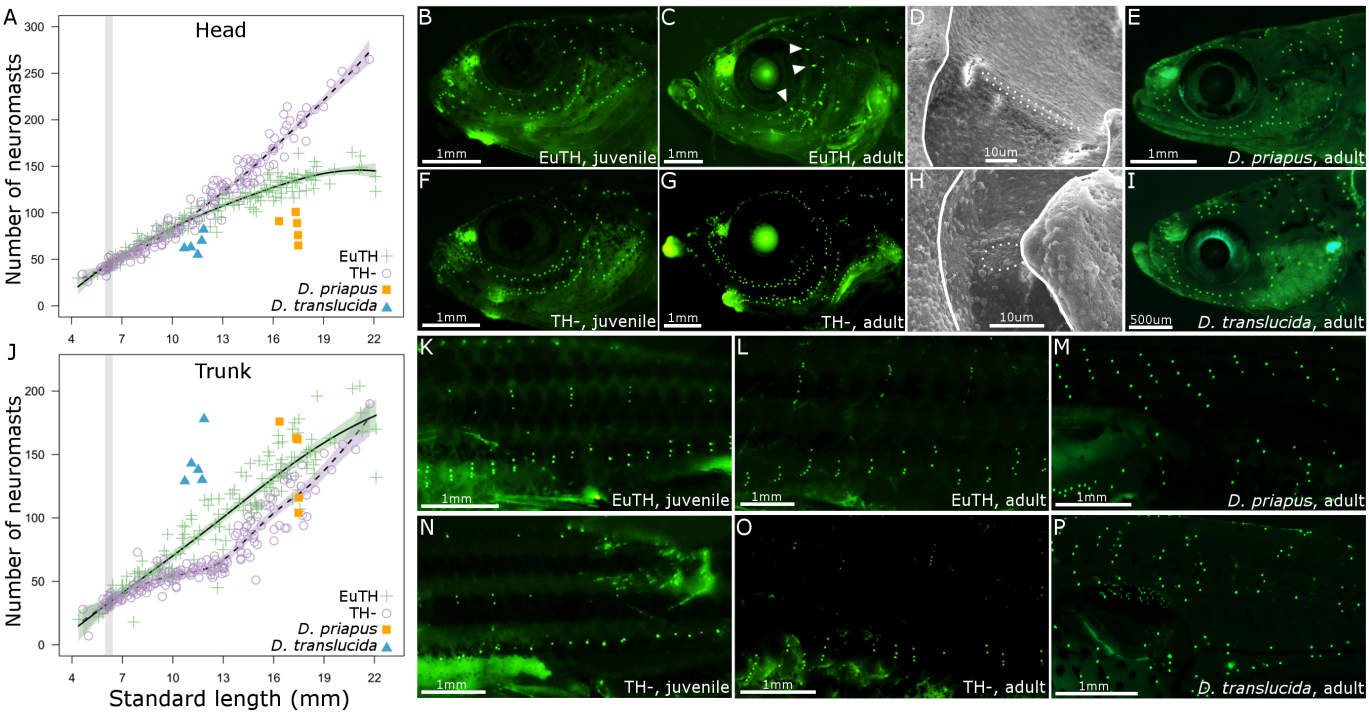
A
Head
Number of neuromasts
EuTH
TH-
D. priapus
D. translucida
J
Trunk
Number of neuromasts
Standard length (mm)
B
EuTH, juvenile
C
EuTH, adult
D
E
D. priapus, adult
F
TH-, juvenile
G
TH-, adult
H
I
D. translucida, adult
K
EuTH, juvenile
L
EuTH, adult
M
D. priapus, adult
N
TH-, juvenile
O
TH-, adult
P
D. translucida, adult

Fig 4

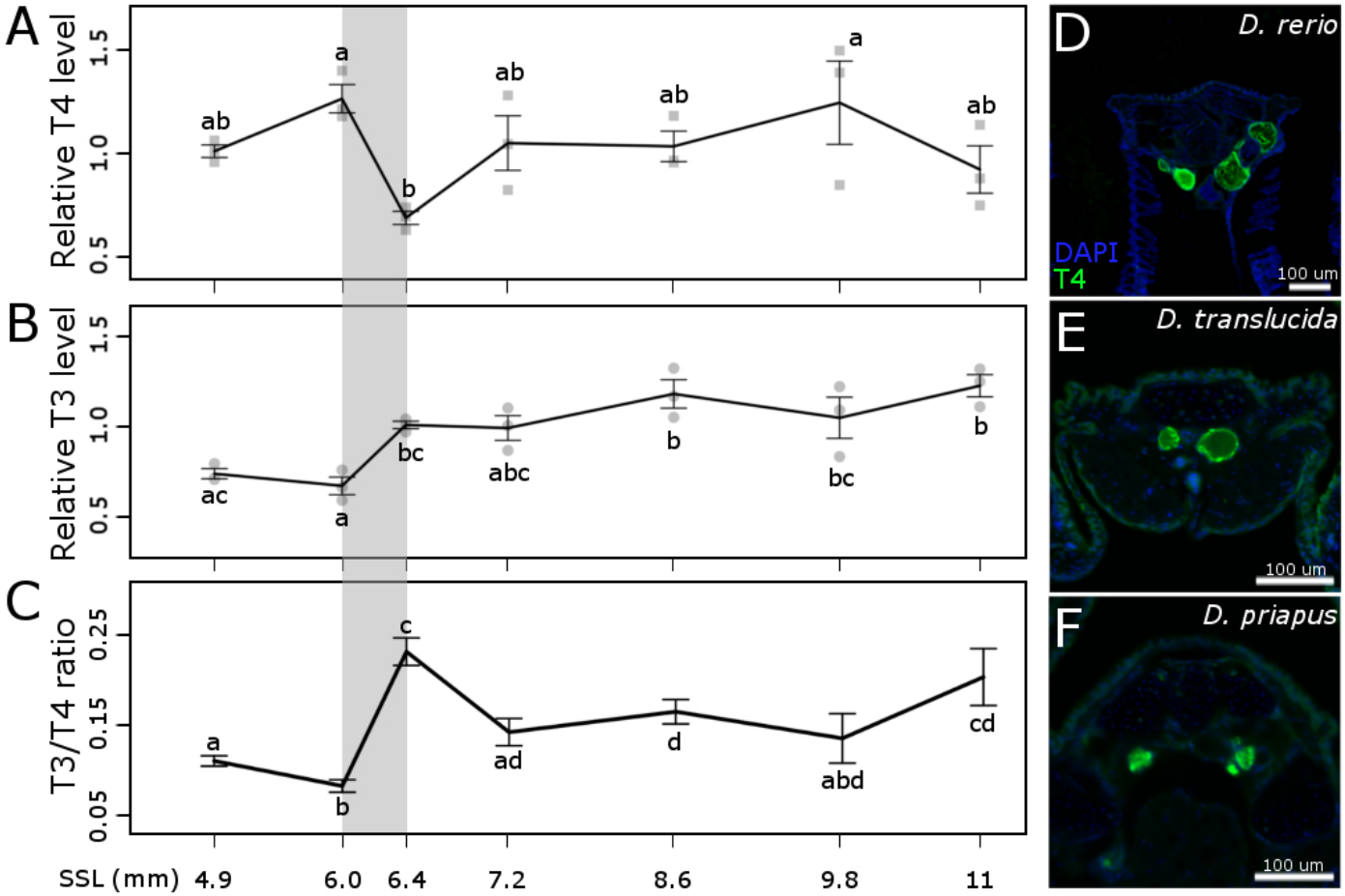
A
Relative T4 level
0.5
1.0
1.5
ab
a
b
ab
ab
a
ab
B
Relative T3 level
0.5
1.0
1.5
ac
a
bc
abc
b
bc
b
C
T3/T4 ratio
0.05
0.15
0.25
a
b
c
ad
d
abd
cd
SSL (mm) 4.9 6.0 6.4 7.2 8.6 9.8 11
D
D. rerio
DAPI
T4
100 um
E
D. translucida
100 um
F
D. priapus
100 um

Supplementary Fig S1

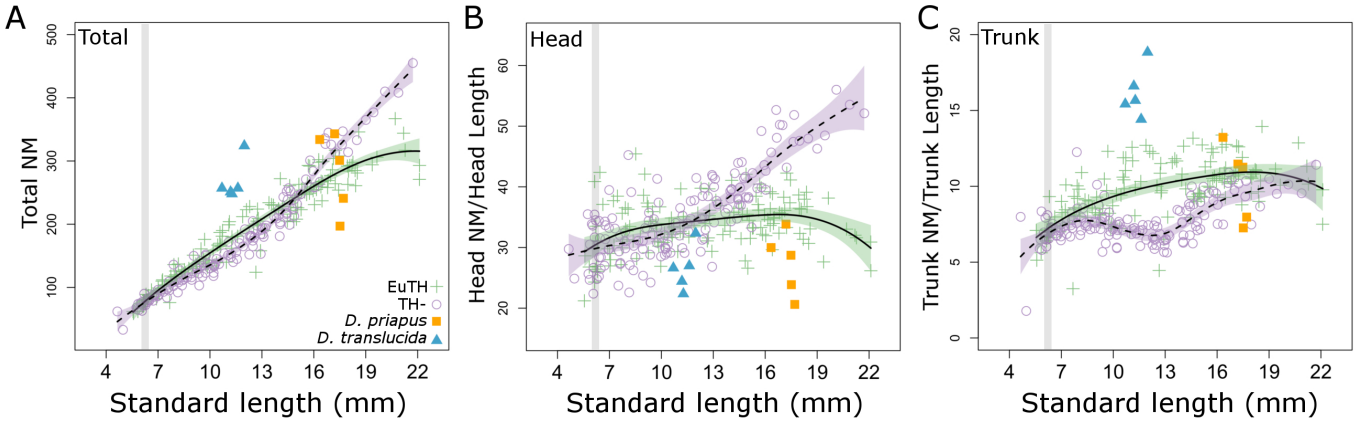

Supplementary Fig S2

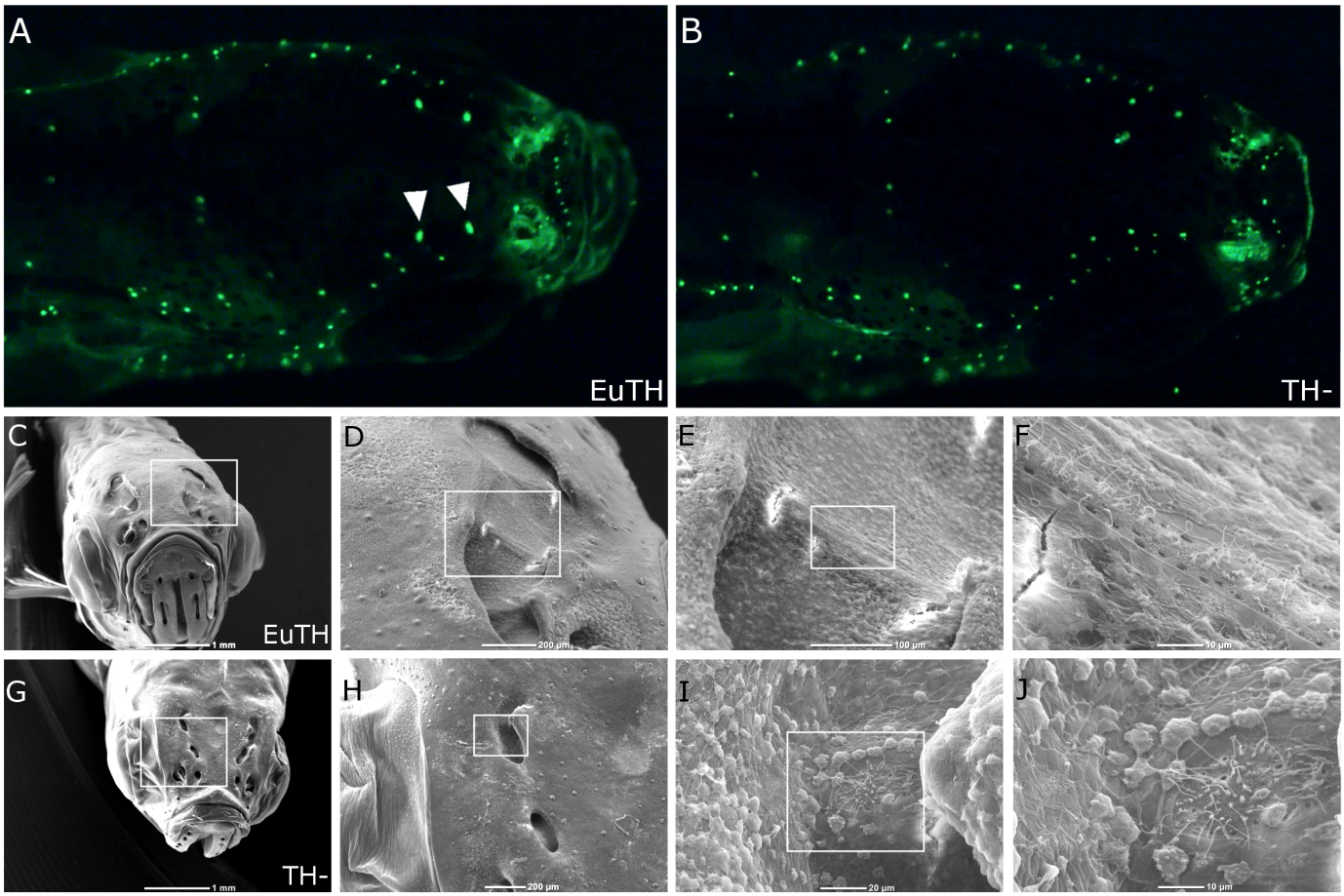

Supplementary Fig S3

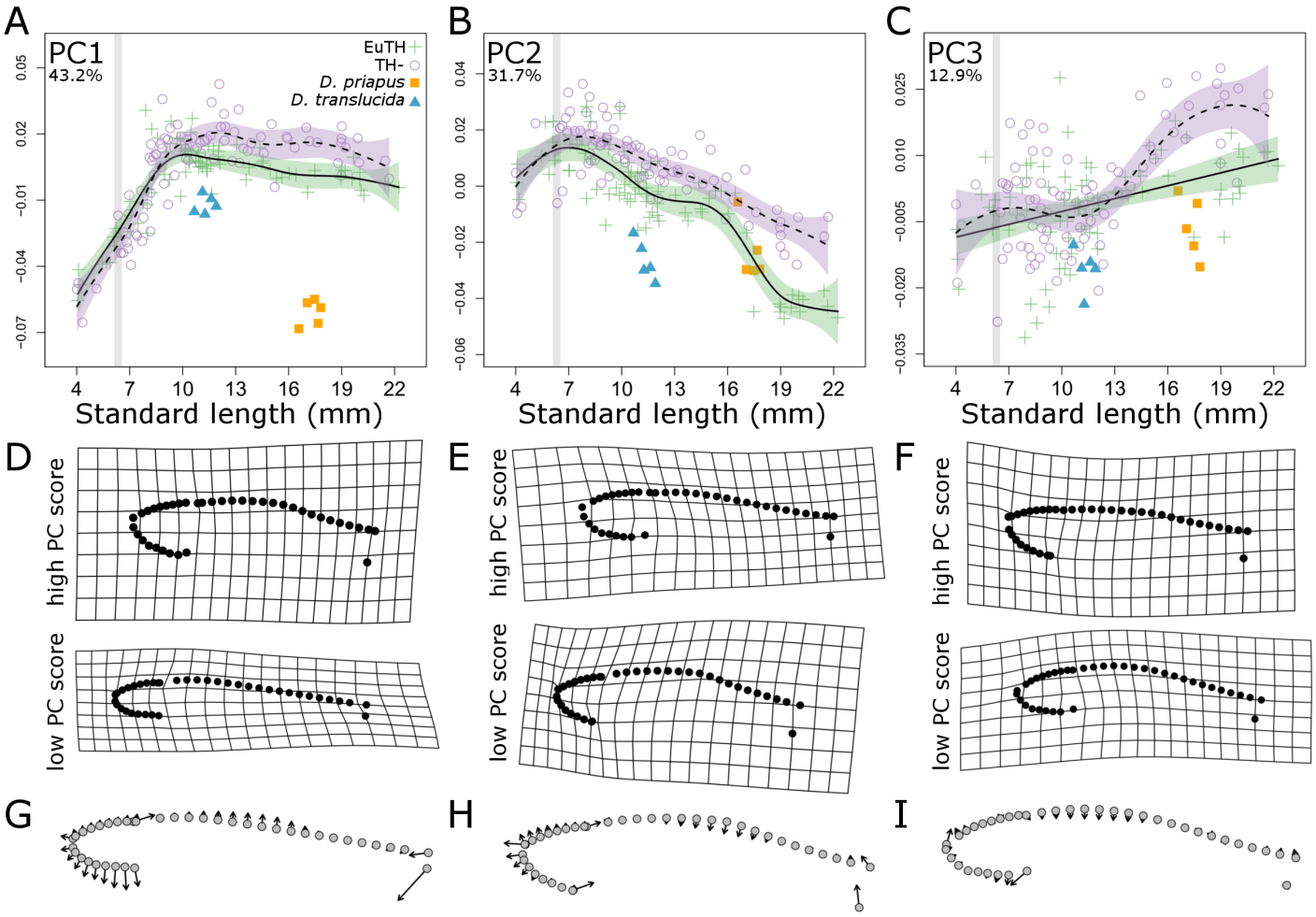
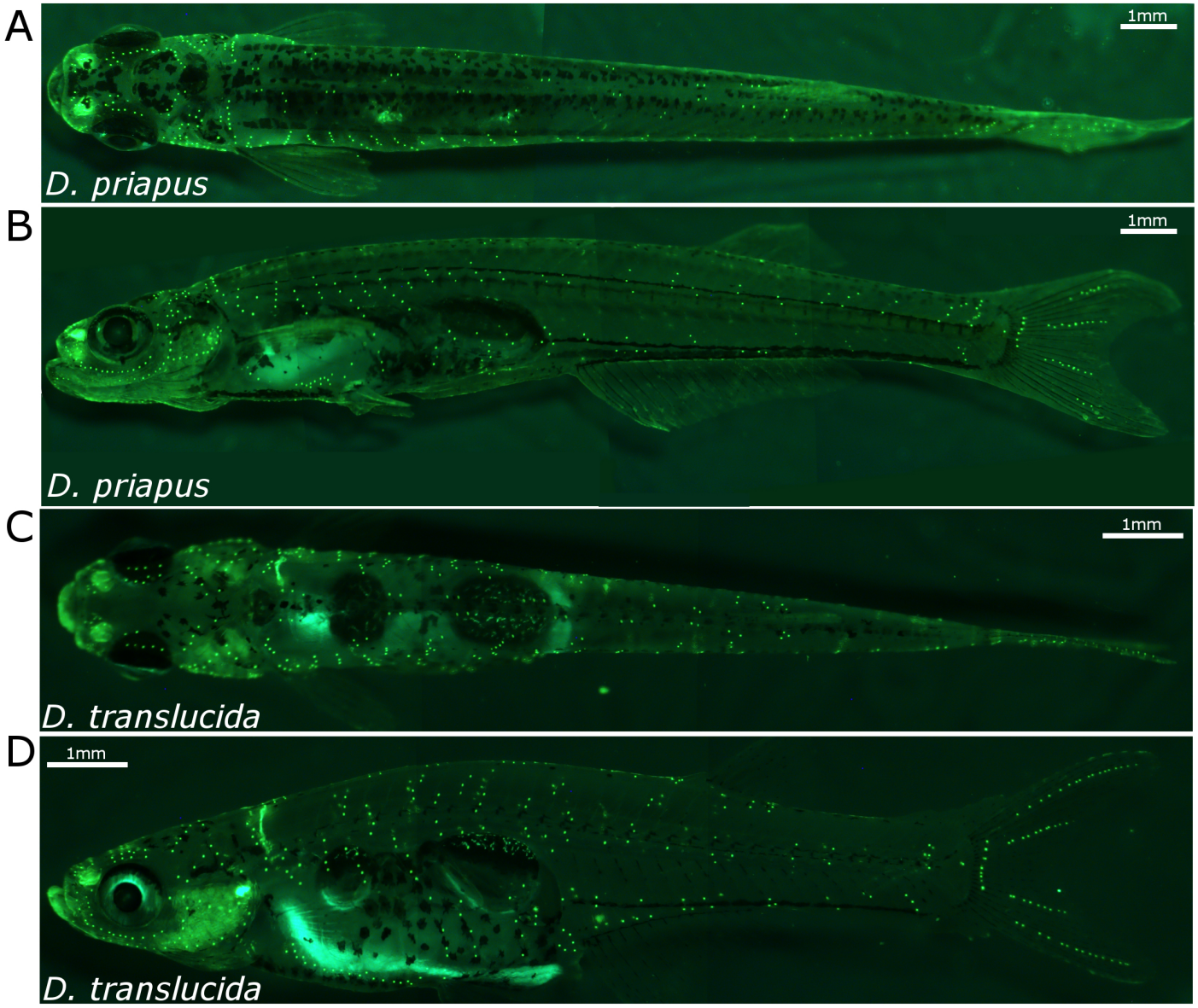
Supplementary Fig S4